Demonstration of high H^- ionic conductivity in barium hydride

Maarten C. Verbraeken[a], Chaksum Cheung[a], Emmanuelle Suard[b] and John T.S. Irvine[a]

[a] *School of Chemistry, University of St Andrews, St Andrews, KY16 9ST, Fife, UK, jtsi@st-and.ac.uk*

[b] *Institut Laue-Langevin, BP 156, 6, rue Jules Horowitz, 38042 Grenoble Cedex 9, France*

With hydrogen being seen as a key renewable energy vector, the search for materials exhibiting fast hydrogen transport becomes ever more important. Not only do hydrogen storage materials require high mobility of hydrogen in the solid state, but the efficiency of electrochemical devices is also largely determined by fast ionic transport. Although the heavy alkaline earth hydrides are of limited interest for their hydrogen storage potential, due to low gravimetric densities, their ionic nature may prove useful in new electrochemical applications, especially as an ionically conducting electrolyte material. Here we show that barium hydride shows fast pure ionic transport of hydride ions (H^-) in the high temperature, high symmetry phase. Although some conductivity studies have been reported on related materials previously, the nature of the charge carriers has not been determined. BaH_2 gives rise to hydride ion conductivity of 0.2 S/cm at 630^{o}C. This is an order of magnitude larger than that of state-of-the-art proton conducting perovskites or oxide ion conductors at this temperature. These results suggest that the alkaline earth hydrides form an important new family of materials, with potential use in a number of applications, such as separation membranes, electrochemical reactors, etc.

Hydride materials have received much interest over the last years for their potential to store hydrogen in the solid state. Because much of the research is aimed at hydrogen storage for onboard applications, such as low temperature fuel cells for the automotive industry, scientists

have focused on finding lightweight materials for optimum gravimetric hydrogen densities[1]. Hence lithium based materials have received a lot of attention, ranging from complex chemical hydrides (e.g. $LiBH_4$ and $LiAlH_4$) to variations of the nitride – imide – amide system [2-4]. The aim has been to find storage materials which show reversible decomposition at low temperatures (typically around 100°C), with fast kinetics. Because of this focus on high gravimetric storage and low thermal stability, hydride materials of the heavier alkali and alkaline earth metals have received little attention over the past 20 years. However, the ionic hydrides in the AeH_2 family (Ae = Ca, Sr, Ba) might prove very useful in understanding the hydrogen mobility and transport in a wide variety of storage materials. And despite their good thermal stability (decomposition at temperatures > 600°C), they show excellent reversibility, which seems to be a common limiting factor for low temperature hydrogen storage materials. Moreover, high temperature applications, such as solid oxide fuel cells for small scale power generation (CHP etc.), may pose stricter requirements on volumetric rather than gravimetric capacity, necessitating the use of storage materials with a better thermal stability than the materials that are typically sought for onboard hydrogen storage. Although these AeH_2 materials' structures are fairly well understood at room temperature, little is known about their structural and transport properties at elevated temperatures. The aim of this study is therefore to gain a better understanding of their high temperature behaviour.

Firstly we consider the structure of BaH_2/BaD_2 between 25°C and 610°C. Peterson et al.[5] reported a phase transition at 580°C which they found using differential thermal analysis techniques. They tentatively associated the high temperature X-ray diffraction pattern with body centred cubic symmetry. The structural change was reversible and the change in diffraction pattern could therefore not be ascribed to the decomposition of barium hydride into barium metal. Their reflections at high temperature however seemed to be of medium

intensity at best, so a more detailed study is necessary to elucidate the high temperature structure of BaH_2. In order to also get information about the positions of the hydride ions, we carried out a neutron diffraction study at variable temperatures showing that BaD_2 has the same cotunnite structure as CaD_2 and SrD_2, which we reported recently[6], at temperature up to ~500°C. The structure has orthorhombic symmetry with spacegroup *P n m a* with Ba and D on three distinct crystallographic *4c* sites (Ba, D1, D2). Our room temperature diffraction data are in good agreement with a previous study by Bronger et al[7]. Also analogous to the previously reported CaD_2 and SrD_2 systems, a significant deuterium substoichiometry was found, which could also be corroborated using thermal analysis (Figure S1 in the supplementary information), resulting in a composition with a large concentration of deuteride vacancies: $BaD_{1.84}$. A minor secondary phase is present, which could be identified as BaO (6.5 mol%, resulting from contamination of the reactants during synthesis and handling). The diffraction patterns of BaD_2 can be refined using this same structural model up to 500°C, when a prominent secondary hexagonal phase emerges, with strongly overlapping peaks. The diffraction pattern at 610°C only shows the hexagonal peaks. The phase change is reversible as the diffraction pattern reverts to the low temperature (<500°C) one as evidenced by the measurement at 250°C upon cooling. Therefore the new phase cannot be attributed to the (partial) decomposition of BaD_2 into barium metal. The diffraction patterns at room temperature and 610°C are shown in Figure 1a, b. In the observed diffraction experiments cotunnite BaD_2 transforms to a hexagonal unit cell, with lattice parameters a = 4.457 Å and c = 6.723 Å, with half the unit cell contents of the cotunnite *P n m a* space-group. Table S1 in the supplementary information lists the actual and ideal *c/b* ratios and atomic coordinates for BaD_2 at room temperature, Figure S2 in the supplementary information also shows the geometrical graphical representation of the relationship between the cotunnite and hexagonal unit cells.

The cotunnite structure of the alkaline earth hydrides, Figure 1c is based on a distorted hexagonal array of alkaline earth ions as can easily be seen by comparing the cotunnite structure with the hexagonal variant in Figure 1d. The BaD_2 structures also involve two D types, D1 which is located at the corner shared vertices between different BaD_x polyhedra and D2 which can be viewed as isolated or only close coordinated to one Ba atom. The ideal hexagonal structure, Figure 1d can be seen as based upon trigonally coordinated layers containing Ba and D1 alternating with layers of D2. The cotunnite structure, Figure 1c is derived from the hexagonal variant by buckling of the BaD1 layers, resulting in a square pyramidal Ba-D coordination involving 3 D1s derived from the trigonal Ba-D1 layer with the addition of a D1 from an adjacent Ba-D1 layer and a D2 from a D2 layer. Whilst all D1s can be viewed as corner shared, the D2 is only in close coordination with one Ba atom. The trigonal arrangement of the Ba-D1 layers in the hexagonal variant is made clear in Figure 1e.

Plotting lattice parameters for the common axis a_{orth} / c_{hex} (Figure S3) or lattice volume (Figure 2) against temperature clearly shows that this phase transition from $P\ n\ m\ a \rightarrow P\ 6_3\ /\ m\ m\ c$ is of first order nature. Due to the co-existence of the two phases at 500°C, refinement of both phases is possible and this clearly shows a discontinuity of said lattice parameters/volume with temperature. The neutron diffraction pattern and refinement at 500°C can be found in supplementary information Figure S6. Peterson's suggested phase diagram also indicates co-existence within a limited temperature range[5]. Despite a slightly smaller lattice volume at room temperature, Figure 2a is in good agreement and complimentary to the low temperature data by Ting et al.[8].

The transition from cotunnite to Ni_2In type structure ($P\ n\ m\ a \rightarrow P\ 6_3\ /\ m\ m\ c$) has been observed before, but in relation to high pressure transformations. This unusual occurrence of

such a high symmetry, high pressure phase in AX_2 compounds was first observed for CaF_2 and SrF_2[9,10], but Tse and Smith later found similar pressure induced cotunnite to hexagonal transformations in CaH_2, SrH_2 and BaH_2[11-13]. Since Tse and Smith's studies were based on X-ray diffraction only, no exact information is available about the positions of the hydride ions at high pressure. So remarkably for AH_2 (A = Ca, Sr, Ba), the cotunnite structure seems to be the preferred structure at ambient conditions, but transforms to the high symmetry Ni_2In type structure at both high temperature and high pressure.

Careful refinement of the neutron diffraction data showed the D1 site in the hexagonal high temperature phase to be split, as shown in Figure 1f. In this hexagonal phase, Ba and D2 occupy the high symmetry *2c* $\left(\frac{1}{3},\frac{2}{3},\frac{1}{4}\right)$ and *2a* $(0,0,0)$ sites, whereas D1 is positioned slightly off the high symmetry *2d* $\left(\frac{1}{3},\frac{2}{3},\frac{3}{4}\right)$ site, on a *4f* site $\left(\frac{1}{3},\frac{2}{3},z\right)$, with *z* being close to 0.83. The displacement from the *2d* site allows expansion of in Ba-D1 distances from 2.57 Å, which is smaller than the smallest Ba-D distance at room temperature, *i.e.* 2.60 Å, to 2.63 Å, see Table S3 for a list of the Ba-D bond distances and Figure S5. The total occupancy of the deuterium sites was fixed to the value obtained from the refinement at 250°C (after cooling down), with the D1 occupancy halved due to the lower site symmetry. The isotropic temperature factors for D1 and especially D2 are remarkably high (7.6 $Å^2$ and 11.6 $Å^2$, respectively). Considering the high temperature and small mass and high mobility of the deuterium ions, this does not seem unreasonable and it might in fact be a clue towards the existence of a superionically conducting regime. It is interesting to note that similar values for the thermal displacements of silver and copper ions were obtained in a high temperature study on the superionic conductors AM_4I_5 (A = Rb, K and M = Ag, Cu)[14].

The refinement further improves upon introducing anisotropy in the thermal displacement of the ions. Especially the D2 site shows highly anisotropic movement in the (002) plane. Figure 2b shows a portion of the unit cell around a barium ion of the hexagonal BaD_2 phase including the thermal ellipsoids, showing this displacement for the D ions. Detailed results of the refinements of BaD_2 at various temperatures can be found in Table S2 and in crystallographic information files.

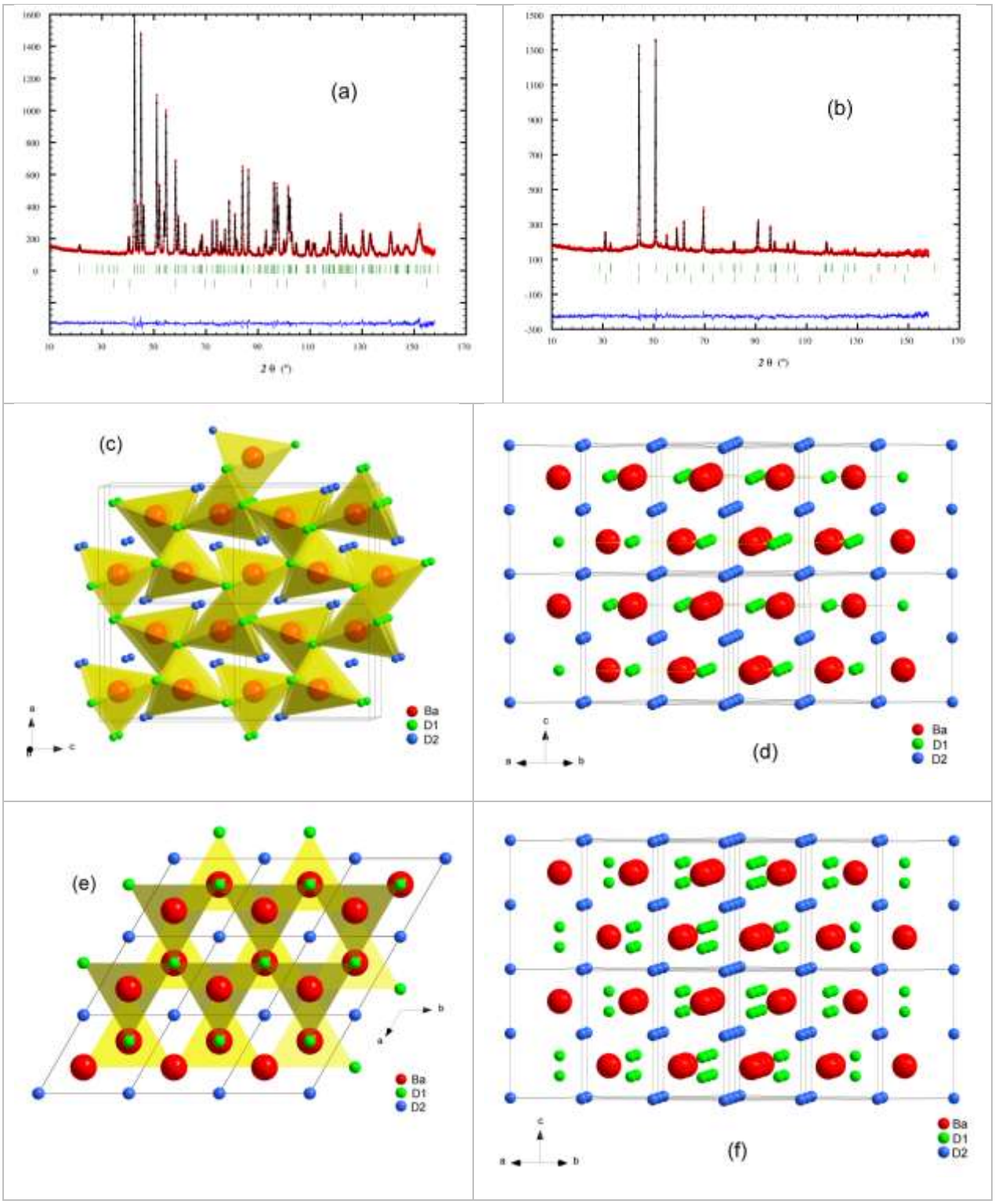

Figure 1: Diffraction patterns for BaD_2 at 25°C (a) and 610°C (b), with representations of the related crystal structures (c, d). The cotunnite structure consists of inverted layers of corner sharing BaD_5 distorted square pyramids (c). Corner sharing is through D1, whereas D2 is only coordinated to one Ba. On going to hexagonal symmetry, a regular layered structure emerges, with alternating Ba-D1 and D2 layers (d). Looking down the c-axis of the ideal hexagonal unit cell shows the trigonal coordination of D1 to Ba (e). The ideal hexagonal structure does not provide the best fit; instead the D1 sites are split and, D1 occupies a partially occupied disordered site resulting in three Ba-D1 bonds of 2.63 Å and one Ba-D1 bonds of 2.84 Å (f).

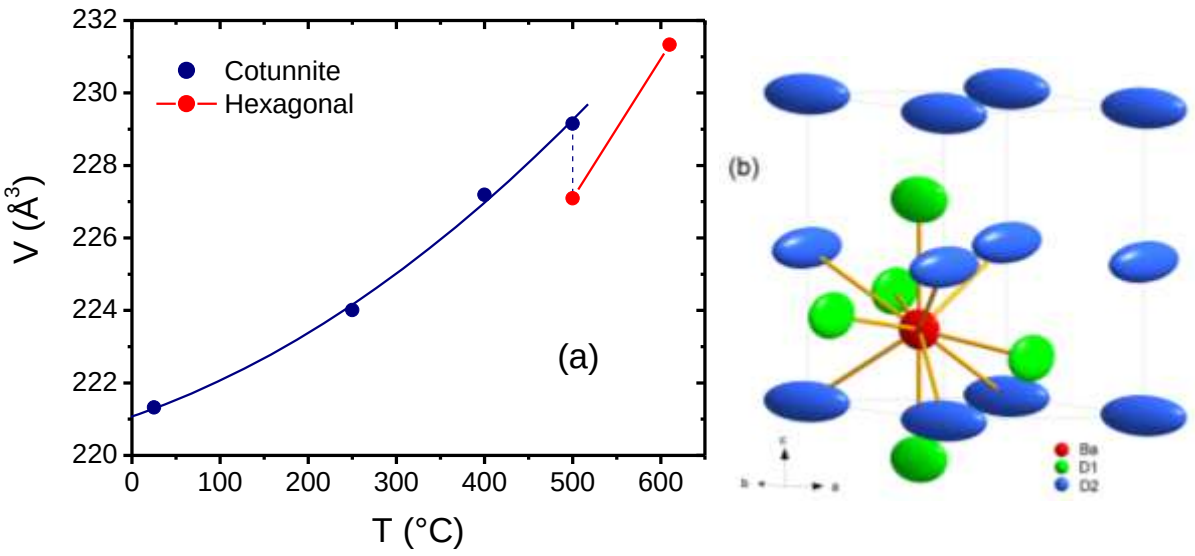

Figure 2: Evolution of lattice volume for BaD_2 with temperature (a). BaD_2 volume shows a 0.9% contraction at 500°C upon going to hexagonal symmetry. Portion of BaD_2 unit cell at high temperature with thermal ellipsoids, showing preferential atomic displacement of D2 site in the *a,b* (002) plane (b)

Previous studies on the electrical behaviour of CaH_2 and SrH_2 showed good conductivity, which is thought to possibly be due to mobility of hydride ions only[6,15]. An increase in conductivity by a factor of 5 – 7 was seen on going from CaH_2 to SrH_2. Following that trend, it is expected that BaH_2 might have even higher conductivity for hydride ions. The high temperature phase transition should be further evident from conductivity studies and possibly give rise to even higher mobility of the hydride ions due to an increase in symmetry. Conductivity data for BaH_2 was examined using electrical impedance spectroscopy. A typical impedance spectrum for BaH_2 recorded at 320°C can be found in Figure 3. It shows the grain boundary response at high frequency and the electrode behaviour at intermediate – low frequency. Deconvolution of the bulk and grain boundary conductivities was possible up to 420°C. For higher temperatures these processes could not be separated anymore as the frequency window was insufficient and total conductivities are reported instead. As the grain

boundary contribution became very small at 420^{o}C, it is reasonable to assume that highest temperature data are also bulk dominated as grain boundaries tend to be more thermally activated than grain interiors. As electrode polarisation resistance started to dominate the impedance at high temperatures increasing the errors in bulk conductivity value determination, and due to risk of structural hydrogen loss, no impedance measurements were taken above 630°C. A detailed description of how the various contributions have been extracted from the impedance data can be found in the supplementary information.

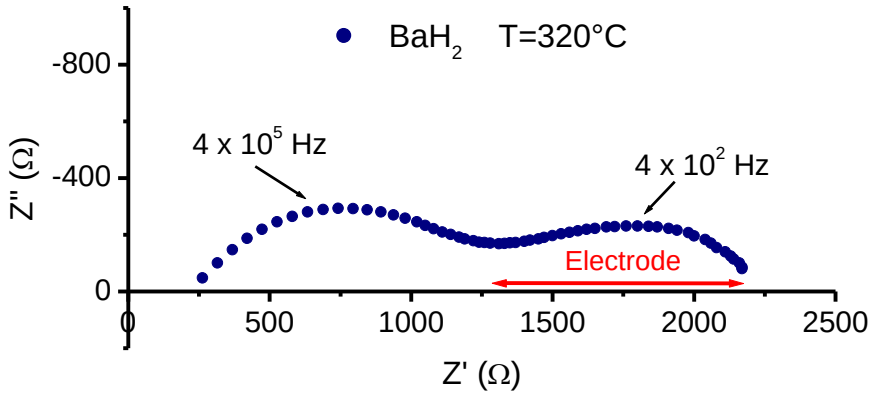

Figure 3: Impedance spectrum of BaH_2 at 320°C, showing grain boundary and electrode response

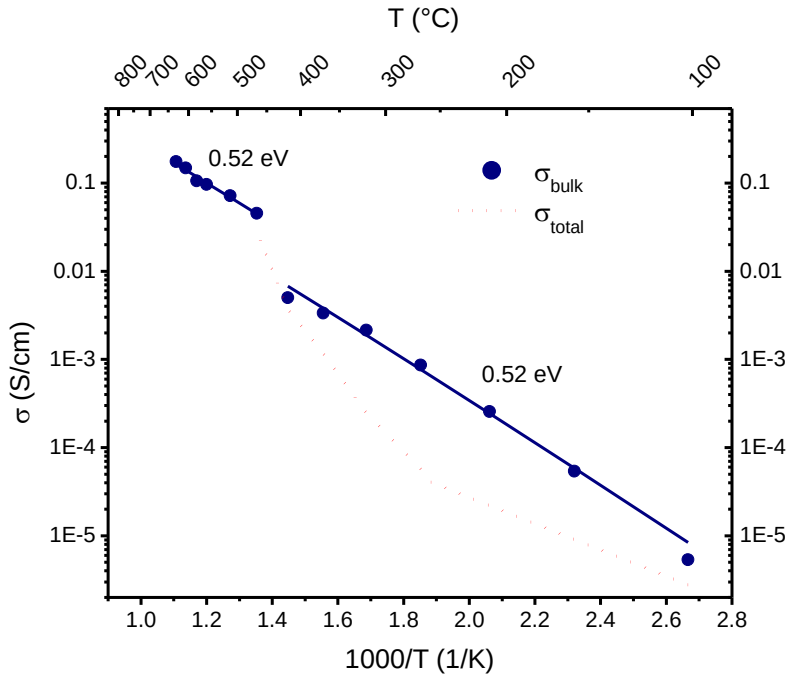

Figure 4: Plot of bulk conductivity for BaH_2, extracted from fitted impedance data up to 420°C. High temperature bulk conductivity was extrapolated from total conductivity data.

An Arrhenius type plot for the bulk conductivity for BaH_2 is shown in Figure 4. The activation energy for bulk hydride ion conduction in the cotunnite structure is 0.52 ± 0.02 eV which is slightly lower than observed for CaH_2 and SrH_2[6], which might be due to the larger Ba ions creating a more open structure for the hydride ions to move and thereby increasing their mobility. When extrapolating the high temperature bulk conductivity, a discontinuity can be observed between 420 – 470°C, leading to an increase in conductivity of approximately an order of magnitude. This sudden jump in conductivity seems to be in good agreement with the onset of the high temperature phase transition as observed in neutron diffraction. Interestingly, the high temperature phase has an activation energy of 0.52 ± 0.03 eV, which is close to the activation energy in the low temperature phase. The total conductivity at 630°C is 0.2 S/cm.

To establish the nature of the observed conductivity data, a dense BaH_2 pellet with Pd electrodes was used as a separating membrane in a concentration cell setup with two different hydrogen containing atmospheres (pH_2' and pH_2"). The voltage across the cell in such a cell will yield an ionic transport number according to:

$$t_{ionic} = \frac{\sigma_{ionic}}{\sigma_{total}} = \frac{E_{obs}}{E_{Nernst}} \quad (1)$$

Where E_{Nernst} is determined by the Nernst equation:

$$E_{Nernst} = -\frac{RT}{nF} \ln \frac{pH_2'}{pH_2''} \quad (2)$$

The partial hydrogen pressures pH_2' and pH_2" were chosen as 1 bar and 0.5 bar respectively, with argon as the balance gas. Whilst using a large difference in partial pressure would give larger voltages, the sensitivity to small leakages causes much instability. Gas flow meters on the reactor outlet confirmed reasonable gas sealing however. The voltages were measured as $E(pH_2') - E(pH_2'')$, (with $pH_2' > pH_2''$). Then according to the half-cell reactions involving hydride ions ($H_2(g) + 2e^- \rightleftarrows 2H^-$), positive voltages are expected. In the case of protonic transport, negative voltage readings would be obtained.

Figure 5 shows two sets of voltages obtained between 475°C and 575°C and the theoretical Nernst voltage for a purely ionic (H^-) conductor. It shows that the high temperature phase gives near theoretical voltages. At temperatures below ~500°C the observed voltage is lower and is less stable. This is possibly due to electronic leakage as resistance of the hydride is

higher at low temperatures and electronic defects may have higher relative higher mobility, or more likely due to gas leakage, as sealing onto these materials improves on heating as the materials become more compliant. As grain boundary contributions and phase changes are not significant in this measured region it seems less likely that the low OCV relates to an alternate conduction species at low temperatures. Predominant ionic conductivity is further confirmed by impedance data at high temperatures, showing a clear electrode response and thus electrochemistry involving the hydride ion, which would have been absent in the case of electronic transport (see Figure S7).

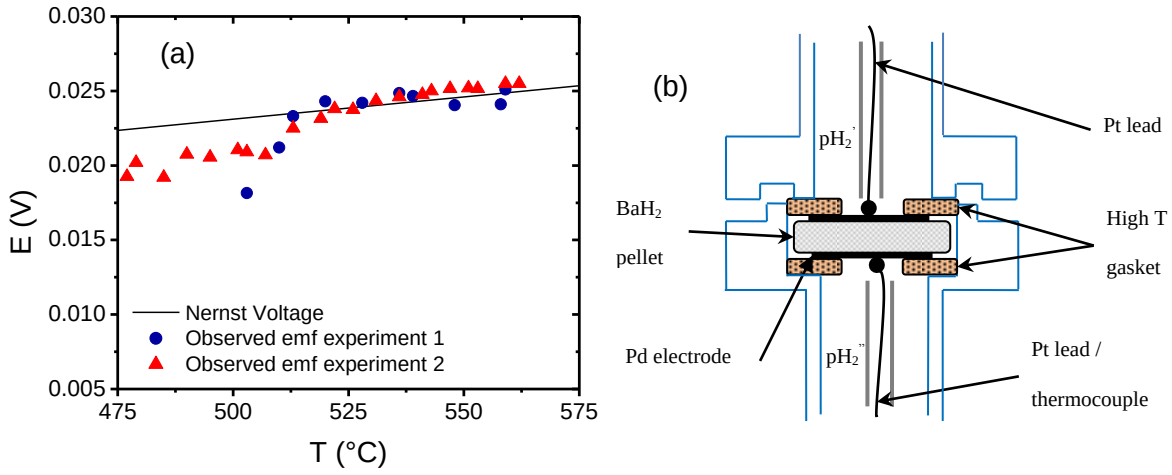

Figure 5: Results for the concentration cell experiment carried out on BaH_2 and experimental setup. The electromotive force (emf) values for two experiments are shown in (a) (red triangles and blue circles) along with the theoretical Nernst voltage (solid line) for the chosen partial hydrogen pressures, pH_2' and pH_2". The setup is shown in (b), consisting of a dense BaH_2 pellet with Pd electrodes, separating the two hydrogen atmospheres.

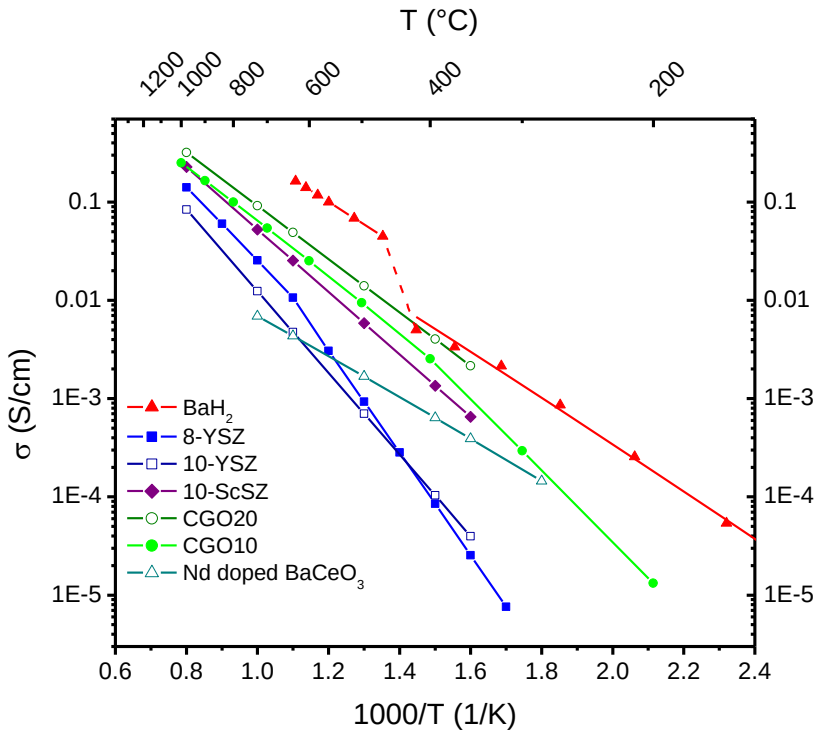

Figure 6: Comparison of bulk conductivities for BaH_2 (▲) and various ionic conductors: (■) 8-YSZ [16], (□) 10-YSZ [17], (◆) 10-ScSZ [17], (●) $Ce_{0.90}Gd_{0.10}O_{1.95}$ [18], (○) $Ce_{0.80}Gd_{0.20}O_{1.90}$ [17], (△) Nd doped $BaCe_{0.90}Nd_{0.10}O_{3-\delta}$ [19]; High temperature (>420°C) data for BaH_2 represents total conductivity; the actual bulk conductivity may therefore be higher.

Not only does BaH_2 show much improved conductivity over its calcium and strontium analogues[6]; its total conductivity is also significantly higher than that of typical good oxide ion and proton conductors such as $Ce_{0.9}Gd_{0.1}O_{1.95}$ and $Ba(Y_{0.1}Ce_{0.9})O_3$ (bulk conductivities of 0.025 S/cm and 0.003 S/cm at 600°C, respectively), even after optimisation of these by co-doping with other elements[18-21], as shown in Figure 6. Furthermore, it is the first material to be clearly demonstrated as having pure hydride ion conductivity. Due to its reactive nature, the hydride ion has the potential to play an important role in electrochemical conversion reactors and other hydrogen related catalytic applications.

Transitions to higher symmetry often lead to lowering of the activation energy for ionic transport. This is not observed for BaH_2, probably indicating that competing factors are cancelling out. Whilst the mobility in the D2 planes would be expected to be greater in the high temperature form, the diffusion in the other direction between these planes may be more difficult. Thus the activation energy in a polycrystalline material may not change; however, the number of available sites for migration is considerably increased on undergoing this transition.

In the orthorhombic symmetry, $H(D)^-$ transport is expected to be in the (102) plane, where the H – H hopping distances are smallest, with 3.1 – 3.2 Å (at 500°C). In the hexagonal phase, the observed large anisotropy in especially the D2 site suggests that conduction of hydride ions is preferentially in the (002) planes of the hexagonal unit cell. The displacement of the D1 site to the lower symmetry *4f* site furthermore enhances this transport, decreasing the D – D hopping distance to 2.8 Å. So despite the thermal lattice expansion, upon going to the high symmetry phase, this hopping distance is reduced by 10 – 13%. Moreover, with the *4f* site half occupied and assuming a vacancy mediated transport mechanism, a large concentration of carriers would be available for ionic transport, resulting in a very conductive phase. This would account for the sudden increase in conductivity at temperatures over 470°C.

The presence of a small amount of BaO (< 1 mol%) in the BaH_2 pellets used for conductivity measurements is not expected to affect the conductivity data presented here. Its solubility is believed to be very small due to the incompatibility of oxide and hydride ions and any doping by this low level of oxide would only cause an insignificant amount of hydride ion vacancies, as compared to the intrinsic concentration. Hydride and oxide ions have been reported to co-exist in certain oxides[22], but for such alkaline compounds as BaH_2/BaO this is thermodynamically very unlikely[23].

Conclusions

A high symmetry phase of BaH_2/BaD_2 was found at temperatures above 500°C and successfully refined using the hexagonal space-group *P 6$_3$ / m m c*. This high symmetry phase gives rise to a sharp increase in the total conductivity, which seems caused by splitting occupation of one hydride site into two sites resulting in a large concentration of charge carriers. The activation energy for hydride ion conduction is 0.52 ± 0.03 eV. Concentration cell experiments showed that hydride ions are the dominant charge carriers in the highly conductive, high temperature phase of BaH_2, but experimental difficulties cannot exclude the possibility of minor contributions from electronic carriers. Compared to oxides, there is a fairly large anion deficiency in prepared barium hydrides, as has previously been reported; however, the resultant charge compensation does not result in significant electronic conductivity. It can therefore be speculated that the resulting defects may be electrons trapped on vacant anion sites as in the well-known F-centres in alkali halide crystals.

Methods

Because of the air and moisture sensitive nature of the reactants and products, all handling was carried out in an argon filled glovebox, unless stated otherwise. BaH_2 and BaD_2 were synthesised by reacting barium metal (Alfa Aesar, 99+%) with hydrogen gas (BOC, High Purity, 99.995%) or deuterium gas (Spectra Gases, 99.995% chemical purity, 99.7% atom enrichment), respectively. The barium metal was loaded in molybdenum crucibles into a stainless steel reactor. The reactor was thoroughly purged with purified argon after which the reaction was carried out at 700°C in flowing hydrogen/deuterium conditions.

Neutron diffraction data were obtained on instrument D1A at Institut Laue-Langevin, ILL (Grenoble, France). The BaD_2 powder sample of approximately 3 grams was loaded into a

vanadium container in a glovebox. A steel cap was fitted on top of the vanadium container, which prevented the sample from decomposing, whilst being transported to the diffractometer. The neutrons had a wavelength of 1.909 Å. Neutron diffraction patterns were recorded between $0 < 2\theta < 158°$ with a resolution of 0.05°, at room temperature (25°C, RT), 250°C, 400°C and 500°C and 610°C, all under vacuum. After heating up to the desired temperature, 20 minutes was allowed for equilibration. The pattern at 250°C was recorded on cooling down to confirm reversibility.

Electrical testing was carried on sintered pellets of BaH_2. It is important to note that the weight gain after synthesis for BaH_2 corresponds to a much reduced amount of secondary BaO phase as observed for the BaD_2 neutron powder sample. It is expected that the level of BaO in the conductivity samples is at least a factor of 10 smaller. Pellets of BaH_2 were pressed at 200 MPa and subsequently sintered at 800°C for 2 hours in pure hydrogen. Palladium paint was applied on both sides of the sintered pellets after which the electrodes were annealed overnight at ~550°C. Impedance spectra in the frequency range of 13 MHz – 5 Hz were recorded with an HP4192A impedance analyser, using an AC perturbation voltage of 100 mV. Annealing and testing were all performed in a 5% H_2 / 95% argon atmosphere. The validity of the impedance data was tested by performing the Kronig Kramers transformation. Kronig Kramers validation ensures the impedance response is within the linear regime and the measured cell is in equilibrium[24]. Electromotive force (emf) values were recorded with increasing temperature on similarly prepared samples in a concentration cell setup, where the 2 – 3 mm thick, dense BaH_2 pellets were separating two different hydrogen atmospheres. Thermiculite (Flexitallic) was used as a gasket sealing material, while the voltages were recorded on a Solartron 7150 multimeter.

References

1 Schlapbach, L. & Zuttel, A. Hydrogen-storage materials for mobile applications. *Nature* **414**, 353-358 (2001).

2 Chen, P., Xiong, Z. T., Luo, J. Z., Lin, J. Y. & Tan, K. L. Interaction of hydrogen with metal nitrides and imides. *Nature* **420**, 302-304 (2002).

3 Zuttel, A. *et al.* $LiBH_4$ a new hydrogen storage material. *J. Power Sources* **118**, 1-7 (2003).

4 Blanchard, D., Brinks, H. W., Hauback, B. C. & Norby, P. Desorption of $LiAlH_4$ with Ti- and V-based additives. *Materials Science and Engineering B-Solid State Materials for Advanced Technology* **108**, 54-59 (2004).

5 Peterson, D. T. & Indig, M. The barium-barium hydride system. *J. Am. Chem. Soc.* **82**, 5645-5646 (1960).

6 Verbraeken, M. C., Suard, E. & Irvine, J. T. S. Structural and electrical properties of calcium and strontium hydrides. *J. Mater. Chem.* **19**, 2766-2770 (2009).

7 Bronger, W., Scha, C. C. & Muller, P. Crystal-Structure of Barium Hydride, Determined by Neutron-Diffraction Experiments on BaD_2. *Zeitschrift Für Anorganische Und Allgemeine Chemie* **545**, 69-74 (1987).

8 Ting, V. P., Henry, P. F., Kohlmann, H., Wilson, C. C. & Weller, M. T. Structural isotope effects in metal hydrides and deuterides. *Physical Chemistry Chemical Physics* **12**, 2083-2088 (2010).

9 Dorfman, S. M. *et al.* Phase transitions and equations of state of alkaline earth fluorides CaF2, SrF2, and BaF2 to Mbar pressures. *Physical Review B* **81**, doi:10.1103/PhysRevB.81.174121 (2010).

10 Wang, J. S. *et al.* Structural phase transitions of SrF2 at high pressure. *Journal of Solid State Chemistry* **186**, 231-234 (2012).

11 Tse, J. S. *et al.* Structural phase transition in CaH_2 at high pressures. *Physical Review B* **75**, - (2007).

12 Smith, J. S., Desgreniers, S., Klug, D. D. & Tse, J. S. High-density strontium hydride: An experimental and theoretical study. *Solid State Commun.* **149**, 830-834 (2009).

13 Smith, J. S., Desgreniers, S., Tse, J. S. & Klug, D. D. High-pressure phase transition observed in barium hydride. *J. Appl. Phys.* **102**, - (2007).

14 Hull, S., Keen, D. A., Sivia, D. S. & Berastegui, P. Crystal structures and ionic conductivities of ternary derivatives of the silver and copper monohalides - I. Superionic phases of stoichiometry MA(4)I(5): RbAg4I5, KAg4I5, and KCu4I5. *J. Solid State Chem.* **165**, 363-371 (2002).

15 Gorelov, V. P. & Pal'guev, S. F. Conductivity in CaH_2 - LiH and CaH_2 - CaF_2 systems. *Elektrokhimiya* **28**, 1294-1296 (1992).

16 Gibson, I. R. & Irvine, J. T. S. Study of the order-disorder transition in yttria-stabilised zirconia by neutron diffraction. *J. Mater. Chem.* **6**, 895-898 (1996).

17 Steele, B. C. H. in *High conductivity solid ionic conductors* (ed T. Takahashi) (World Scientific Publishing Co. Pte. Ltd, 1989).

18 Steele, B. C. H. Appraisal of Ce1-yGdyO2-y/2 electrolytes for IT-SOFC operation at 500 degrees C. *Solid State Ionics* **129**, 95-110 (2000).

19 Chen, F. L., Sorensen, O. T., Meng, G. Y. & Peng, D. K. Preparation of Nd-doped BaCeO3 proton-conducting ceramic and its electrical properties in different atmospheres. *J. Eur. Ceram. Soc.* **18**, 1389-1395 (1998).

20 Omar, S., Wachsman, E. D. & Nino, J. C. Higher conductivity Sm3+ and Nd3+ co-doped ceria-based electrolyte materials. *Solid State Ionics* **178**, 1890-1897 (2008).

21 Norby, T. Solid-state protonic conductors: principles, properties, progress and prospects. *Solid State Ionics* **125**, 1-11 (1999).
22 Hayward, M. A. *et al.* The hydride anion in an extended transition metal oxide array: LaSrCoO3H0.7. *Science* **295**, 1882-1884 (2002).
23 Norby, T., Wideroe, M., Glockner, R. & Larring, Y. Hydrogen in oxides. *Dalton T*, 3012-3018 (2004).
24 Boukamp, B. A. A Linear Kronig-Kramers Transform Test for Immittance Data Validation. *J. Electrochem. Soc.* **142**, 1885-1894 (1995).

Acknowledgements

We thank EPSRC for support through a Platform Grant, the Royal Society for a Wolfson Merit award and ILL for provision of neutron beam time.

Author Contributions

Verbraeken contributed significantly to all aspects. Cheung to synthesis and characterisation, Suard to neutron diffraction and Irvine to concept and manuscript.